Comparison of two typhoon-induced storm surges at the Zhanjiang Coast

Xue Zhao[1], Qiang Xie[2], Bo Hong[3*], Hongzhou Xu[2], Lingfang Chen[2], Jinlei Hu[1], Min Zhang[1], Baoxia Huang[1], Zhiwei Che[4]**

[1]South China Sea Forecast Center, State Oceanic Administration, Guangzhou, Guangdong 510310, China

[2]Institute of Deep-sea Science and Engineering, Chinese Academy of Sciences, Sanya, Hainan 572000, China

[3]School of Civil and Transportation Engineering, South China University of Technology, Guangzhou, Guangdong 510641, China

[4]Haikou Marine Environment Monitoring Center Station, State Oceanic Administration, Haikou, Hainan 570311, China

*Equal to the first author
**Corresponding author: hzxu@sidsse.ac.cn

Abstract. Typhoon-induced storm surge is the largest threat to the Zhanjiang Coast of the northern South China Sea. In this study, we report on two processes of storm surges generated by Typhoons Rammasun (TR) and Kalmaegi (TK) with similar tracks at this region. Results show that the peak of the storm surge during TK (with a maximum value of 4.50 m) was significantly larger than that during TR (with the maximum value of 2.60 m), although the intensity of TK (Category 4 with 40 m s^{-1} maximum wind and 960 hPa central air pressure) was much weaker than that of TR (Category 6 with 60 m s^{-1} maximum wind and 910 hPa central air pressure). Comparisons of the typhoon properties and astronomic tides reveal that the peaks of storm surge were closely related to typhoon maximum wind radius, typhoon moving speed, and tide-surge interaction rather than typhoon intensity during the two cases, indicating complex dynamics of storm surge at the Zhanjiang Coast.
Keywords: Storm surge, Typhoon, Wind radius, Moving speed, Zhanjiang Coast

1. Introduction

The storm surge hazard induced by landing typhoons in Asia and hurricanes in North America (both are named typhoon in this study) has become a serious threat to the coastal ecological environment and its dynamics have been studied for several decades. Weisberg and Zheng (2006) pointed out that the intensity of a typhoon is a key factor for determining the strength of the storm surge in the Tampa Bay off the Florida coast based on numerical simulations. Their result indicated the height of the storm surge was proportional to the square of the wind speed in the Tampa Bay. Powell and Reihold (2007) also suggested storm surge can be estimated by kinetic energy of a typhoon based on the analyses of the relation between storm surge and typhoon kinetic energy during several typhoons in North America.

Proudman (1953) concluded that the moving speed of a typhoon has an important impact on the peak of the storm surge, in which storm surge reached maximum value when the moving speed was close to the propagation speed of its long wave. Rego and Li (2009) studied the responses of storm surge to hurricanes with different moving speeds at the coasts of Louisiana and pointed out that typhoons with faster moving speeds can indeed cause higher surges, but with faster dissipation rates. A similar phenomenon has also been found in the Florida Bay (Zhang et al., 2012). However, the peaks of storm surges are reduced by typhoons with faster moving speeds in some areas with complex topography, such as the Tampa Bay in Florida (Weisberg and Zheng, 2006), North Carolina coasts (Peng et al., 2004), and Hangzhou Bay (Han and Pan, 2013), where the propagation speed of long waves is smaller than the moving speed of the typhoons. Xu et al. (2010) found the peaks of storm surges were determined by typhoon tracks around the Florida coasts and found that topography with half-closed bay and estuary more easily allowed for accumulation of the water column. Han and Pan (2013) found different typhoon tracks caused largely different storm surges at the Hangzhou Bay. In addition, the shallow continental shelf is favorable for formation of a storm surge, as the surge wave is upraised suddenly when it runs up against the shallow topography (Rego and Li, 2010). The above studies indicate that the peak of a typhoon-induced storm surge

is dependent on a number of factors and the dynamics are very complex.

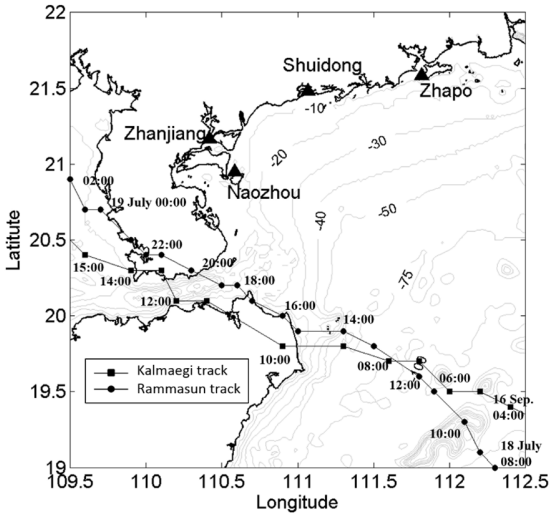

Figure 1. Tracks of TK (squared line) and TR (dotted line). Triangles represent tide-gauge stations at Naozhou, Zhanjiang, Shuidong and Zhapo. Black and gray lines represent coastline and isobaths at the Zhanjiang Coast, respectively.

The Zhanjiang Coast is located on the west coast of Guangdong Province (Figure 1). It connects with the northern South China Sea through a wide and shallow shelf which extends about 230 km from the coastline to 100 m water depth. Its shallow and half-closed shelf makes the Zhanjiang Coast one of the most storm-surge prone areas along China's coastline (Elliott et al., 2015). Dong et al. (2014) studied the temporal and spatial distributions of storm surges along the Guangdong Coasts using a 50-year dataset at ten tide gauge stations and concluded that the Zhanjiang Coast was the most severely affected area with the highest frequency of storm surges. There is no doubt that different typhoons can cause different levels of storm surge along the Zhanjiang Coast. For example, Typhoon 8007, which was a Category 4 storm, caused a 5.90 m storm surge at Nandu tide gauge station along the Zhanjiang Coast, while Typhoon Krovanh, another Category 4 storm, and Typhoon 6508, rated a Category 6, only caused about 3.80 m and 2.40 m storm surges at the same place, respectively (Chen et al., 2002; Shi et al., 2004; Cao et al., 2006). All of the above studies suggest that the height of storm surge was closely related to typhoon intensity, track, and landing location along the Zhanjiang Coast. In this study, we report storm surge processes during two different typhoons with similar tracks and landing locations, but with different intensity, and discuss the potential dynamic mechanisms for the processes at this region. The flow chart of research methodology is showed in Figure 2.

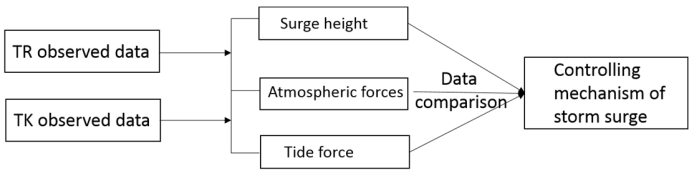

Figure 2. Flow chart of research methodology.

2. Typhoons Rammasun and Kalmaegi

Typhoon Rammasun (TR) initially formed as a tropical depression at about 210 km west of Guam in the Northwestern Pacific at noon of 12 July, 2014. It moved westwards and landed in the central coast of the Philippines after intensifying as a severe typhoon on 15 July. TR entered the South China Sea on 16 July and developed as a super typhoon with maximum 55 m s^{-1} sustained winds and 930 hPa air pressure on 18 July. It moved northwestward and made landfall near Wenchang over the northern Hainan Island at 15:00 on 18 July, becoming the strongest landing typhoon (with 60 m s^{-1} maximum wind and 910 hPa central air pressure) in China since 1949. Seven hours later, it crossed over the Leizhou Peninsula and entered into the Beibu Gulf. It continued to move northward and crossed over Guangxi on 19 July, after weakening to a Category 2 typhoon.

Figure 3. Damages and huge storm surge caused by TR (a) and TK (b), respectively.

Typhoon Kalmaegi (TK) initially generated as a tropical depression about 1100 km southeast of Manila in the Philippines at 14:00 on 12 September, 2014. It rapidly developed into a tropic storm, moving northwest, and then strengthened into a

typhoon with 30 m s^{-1} peak winds and 980 hPa air pressure at about 7:00 on 13 September. TK crossed over the Luzon Island and entered into the South China Sea at midnight on 15 September. The intensity of TK remained at almost the same level, with 40 m s^{-1} maximal winds and 960 hPa air pressure, as it drifted northwestward toward the Hainan Island. Like TR, TK also made landfall near Wenchang at 10:00 on 16 September and then moved northwestward across the Leizhou Peninsula and Beibu Gulf. It finally landed at Hatrang in Vietnam at 23:00 on 16 September.

It can be seen that TR and TK had similar tracks and landing places but largely different intensities and shapes. At landing time, TR reached a Category 6 with 60 m s^{-1} maximal winds and 910 hPa air pressure, while TK reached Category 4 with 40 m s^{-1} maximal winds and 960 hPa air pressure (Figure 4). They both caused severe damage to the China coasts. TR killed at least 62 people and caused 37000 houses collapses and an economic loss of about US$ 6.25 billion. TK killed at least eight people and caused 1800 houses collapse and an economic loss of about US$ 55.86 million. Figure 3 show house damages and surge at the Zhanjiang Coast during TR and TK, respectively.

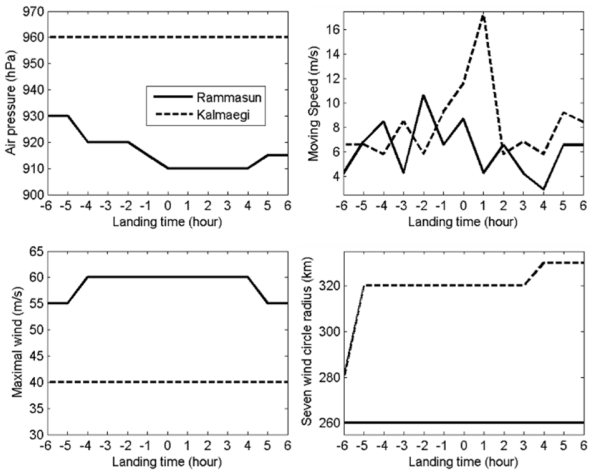

Figure 4. Central air pressure, moving speed, maximum wind, and seven wind circle radius during TR (solid lines) and TK (dashed lines) before and after landing time.

3. Storm Surge Comparison

TR and TK both generated storm surges along the Zhanjiang Coast when they landed at Wenchang. Figure 5 shows the instantaneous (hourly) storm surges, tides, wind speeds, and air pressures during the two typhoons at the Zhapo, Shuidong, Zhanjiang, and Naozhou tide gauge stations along the Zhanjiang Coast. It can be seen that TR caused the highest storm surge at Naozhou, where the peak of the storm surge reached 2.60 m. Surprisingly, the maximum storm surge of 4.50 m was caused by TK at the same tide gauge station, although the intensity of TK (Category 4) was much weaker than TR (Category 6). Higher peak surges also have been found at Zhanjiang (4.35 m), Shuidong (3.00 m), and Zhapo (2.20 m) during TK, compared with those during TR (2.56 m, 1.60 m and 1.15 m, respectively), indicating the height of the storm surges was not proportional to the typhoons' intensity in some cases along the Zhanjiang Coast. We provide specific analyses about why the weaker TK caused a much higher storm surge compared with the stronger TR in the discussion section.

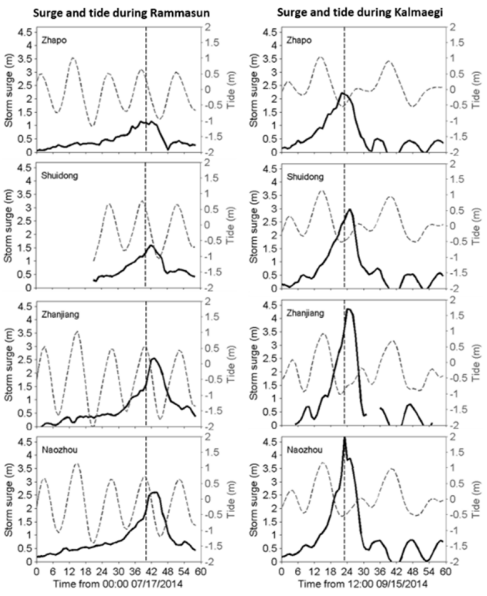

Figure 5. Storm surge (solid lines) and tide (dashed lines) at the Zhapo, Shuidong, Zhanjiang and Naozhou tide gauge stations along the Zhanjiang Coast during TR (left panel) and TK (right panel). Vertical dashed lines represent landing times.

4. Discussion

4.1. Atmospheric forcing

It is well known that height of a storm surge is proportional to the square of wind speed:

$$\eta \propto w^2/H, \qquad (1)$$

in which η and w are the surge height and wind speed, respectively (Powell and Reihold, 2007). Figures 6 shows that the peak wind speeds (minimum air pressures) of TK were much larger (lower) than that of TR at all tide gauge stations along the Zhanjiang Coast. In addition, all the tide gauge

stations were located at the northwest of the typhoon centers before landing time, which made the wind direction similar. Figure 7 shows that wind direction switched from the northern direction to the northeastern direction at all tide gauge stations during TR and TK, which paralleled the shelf of the Zhanjiang Coast and was favorable for the Ekman transport of water mass toward the shore. These results indicate that the larger wind speeds and lower air pressures possibly contributed in some way to the higher surge during TK. The question of why atmospheric forcing during the lower category TK storm was stronger than that of the higher category TR storm at these tide gauge stations can be explained by the distribution of their maximum wind circle radii. Jelesnianski et al. (1992) purposed a formula for calculating the wind speed profile of a stationary storm, which is described as:

$$V_r = V_{max} \times (2 \times R_{max} \times r)/(R_{max}^2 + r^2), \quad (2)$$

in which V_{max} is the maximum wind speed, r is the radius, and $R_{max}$is the radius of maximum wind. The formula for the air pressure profile is the same as for the wind. The authors suggested that the wind speed and air pressure in the outer circle of a typhoon are not only determined by typhoon intensity, but also by the typhoon maximum wind radius. It can be seen that TR and TK had similar ten wind circle radii at between 140 and ~160 km (not shown). However, TK had a much larger seven wind circle radius (about 320 km) than that of TR (about 260 km) (Figure 4), which suggests the power of TR was weakened much faster than that of TK when the wind circle extended outward to these tide gauge stations along the Zhanjiang Coast. As a result, more severe atmospheric conditions occurred at this region during TK.

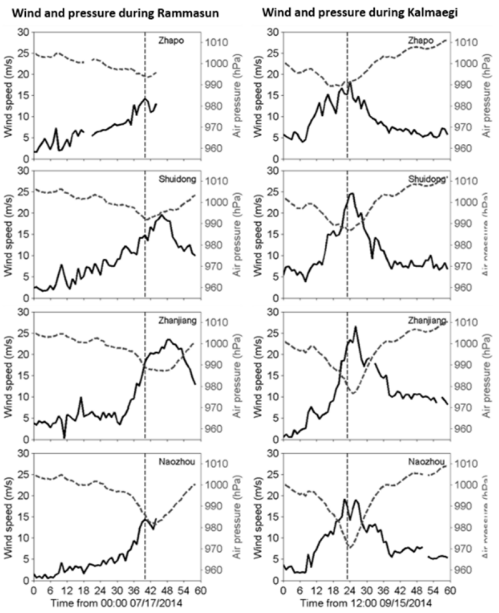

Figure 6. Wind speed and air pressure at the Zhapo, Shuidong, Zhanjiang, and Naozhou tide gauge stations along the Zhanjiang Coast during TK (solid lines) and TR (dashed lines). Vertical dashed lines represent landing times.

4.2. Typhoon moving speed

Proudman (1953) suggested storm surges reach maximum value when the moving speed is close to the propagation speed of the long wave, i.e.

$$\frac{1}{1-\frac{U^2}{gh}} \to \infty, \quad (3)$$

in which U is the typhoon moving speed and $\sqrt{gh}$ is the long wave propagation speed. The mean depth of the Zhanjiang Coast is about 25 m and its long wave propagation speed is about 15.8 m s^{-1}. Figure 4 shows that TR and TK had similar moving speeds (about 7 m s^{-1}) at 1 hour prior to landing. After that, TK suddenly accelerated and its moving speed increased to 15 m s^{-1} at 1 hour after landing at the Wenchang. This was very close to the long wave propagation speed. Conversely, TR decelerated very fast to about 4 m s^{-1} at 1 hour after landing at the Wenchang, a speed that was much smaller than the long wave propagation speed. As a result, a much higher storm surge was generated along the Zhanjiang Coast during TK compared with that of TR. This phenomenon also has been found at other worldwide coastal areas (Rego and Li, 2009; Zhang et al., 2012). Note that the storm surge was generated and dissipated much quicker during TK than TR. Figure 5 shows that the time for storm surge generation from zero to peak was about 24 hours and reduced from peak to zero in about 6 hours during TK. But these times were more than 42 hours and 12 hours for TR, respectively. These results suggest that typhoon with faster moving speed can fleetly cause higher storm surge, but the storm surge declines quicker after its passing through the Zhanjiang Coast.

4.3. Tide–surge interaction

Tide–surge interaction has been recognized for the past half century. Tide not only affects the storm surge height, but also changes the storm surge phase through linear and nonlinear interactions (Rossiter, 1961; Wolf, 1978; Jone and Davies, 1998; Shen et al., 2006; Rego and Li, 2010, Xu et al., 2010). Usually,

flood tide produces higher storm surges compared with ebb tide, and the linear superposition of storm surge and tide can represent total water elevation during typhoons in coastal regions (Proudman, 1957). In this study, we separate the tide and storm surge to see how tide impacted the storm surge during TR and TK. Figure 5 shows that the storm surge reached its peak at the ebb period of spring tide during TR, and the declining tide retarded the development of the storm surge and reduced the total water level along the Zhanjiang Coast. Contrarily, storm surge reached its maximal value at the flood period of neap tide during TK, and the rising tide had a positive effect on development of the storm surge in this region. It is understood that the effect of nonlinear tide–surge interaction on the height of a storm surge is mainly due to alteration of bottom friction. Positive tide increases the total water level and reduces bottom friction, which is constructive to storm surge, while negative tide does the opposite (Davies et al. 2000; Xu et al., 2010). Figure 5 shows that tide level was higher than the mean water level, which increased total water depth and reduced bottom friction during TR. The tide level during TK was lower than the mean water level, which decreased total water depth and added bottom friction, suggesting that the nonlinear tide–surge interaction was destructive to the storm surge during this period. However, how much impact of the nonlinear tide–surge interaction had on storm surge during the two typhoons is unable to be estimated by currently observed results. To explore this, more studies using numerical models will be needed in the near future.

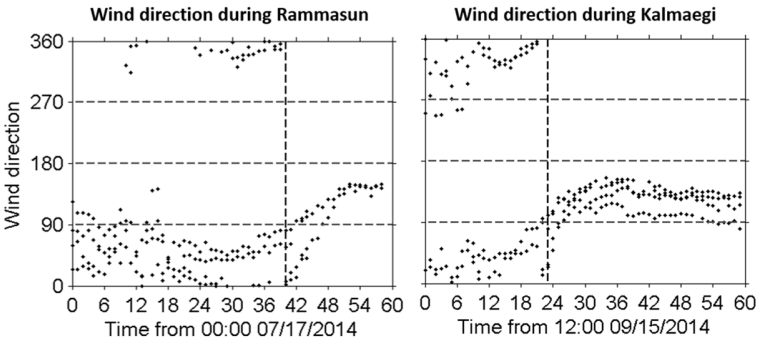

Figure 7. Wind directions (degree) at all four gauge stations during TR and TK. Direction 0, 90, 180 and 360 represent northern, eastern, southern and western winds. Vertical dashed lines represent landing times.

5. Summary

The distributions and propagation processes of storm surges along the Zhanjiang Coast during TR and TK are reported in this study. We find that the peak of the storm surge during TK was significantly larger than that of TR in this region, although the intensity of TK was much weaker than TR. The question of why a higher storm surge was generated during TK than TR can be answered by the three combination of three factors : 1) The power of TK was weakened when the maximum wind circle extended outward to the Zhanjiang Coast, causing stronger winds and lower air pressure during TK compared with TR in this region; 2) the moving speed of TK was closer to the long wave propagation speed compared with TR, which is a favorable factor for high storm surge; and, 3) TR passed by the Zhanjiang Coast during flood tide, which increased its storm surge, while TK passed by this region during ebb tide, which reduced its storm surge. Although the tide–surge nonlinearity had negative and positive effects on the storm surge during TK and TR, respectively, it may have played only a minor role during these processes. To understand speficic impacts of these factors on storm surge along the Zhanjiang Coast, numerical study will be applied in our future work.

Funding Statement

This work was funded by the Knowledge Innovation Program of the Chinese Academy of Sciences under Grants SIDSSE-201306 and SIDSSE-201205, the National Natural Science Foundation of China under Grants 41406005, and the “Hundred Talents Program” of the Chinese Academy of Sciences under Grant SIDSSE-BR-201304 and Y410161KYF.

References

[1] Cao, J.F., Wu, D.P., Lang, X.B., 2006. The storm surge analysis on Typhoon “Krovanh”. Marine Forecasts. 23(2), 63-66.
[2] Chen, Y.D., Dong, Z.J., Jiang, G.R., Luo, J., 2002.Characteristic analysis of Zhanjiang Harbor’s storm surge. Marine Forecasts. 19 (3), 44-52.

[3] Davies, A.M., Kwong, S.C.M., Flather, R.A., 2000.On determining the role of wind wave turbulence and grid resolution upon computed storm driven currents. Continental Shelf Research. 20(1), 825–1,888.
[4] Dong, J.X, Li, T., Hou, J.M., Yu, F.J., 2014. The characteristics of temporal and spatial distribution of storm surge in Guangdong Province and storm surge hazard study at Yangjiang City. Acta Oceanologica Sinica (in Chinese). 36(3), 83-93.
[5] Elliott, R.J.R., Strobl, E., Sun, P., 2015. The local impact of typhoons on economic activity in China: A view from outer space. Journal of Urban Economics. 88, 50–66.
[6] Han, S.Z., Pan, S., 2013. Numerical Simulation and Analysis of Storm Surge in the Hangzhou Bay. Periodical of Ocean University of China. 43(7), 1-6.
[7] Jelesnianski, C.P., Chen, J., Shaffer, W., 1992. SLOSH: Sea, Lake, and Overland Surges from Hurricane. National Weather Service, Silver Springs, MD, (71p).
[8] Jones, J.E., Davies, A.M., 1998. Storm surge computations for the Irish Sea using a three-dimensional numerical model including wave–current interaction. Continental Shelf Research. 18(2), 201–251.
[9] Peng, M.C., Xie, L.A., Pietrafesa, L.J., 2004. A numerical study of storm surge and inundation in the Croatan–Albemarle–Pamlico Estuary System. Estuarine, Coastal and Shelf Science. 59(1), 121-137.
[10] Powell, M.D., Reinhold, T.A., 2007.Tropical cyclone destructive potential by integrated kinetic energy. Bulletin of the American Meteorological Society. 88(4), 513-526.
[11] Proudman, J., 1957. Oscillations of tide and surge in an estuary of finite length. Journal of Fluid Mechanics. 2(4), 371–382.
[12] Proudman, J., 1953. Dynamical Oceanography. John Wiley, New York, 409.
[13] Rego, J.L., Li, C., 2009. On the importance of the forward speed of hurricanes in storm surge forecasting: A numerical study. Geophysical Research Letters. 36(7), doi:10.1029/2008GL036953.
[14] Rego, J.L., Li, C., 2010. Nonlinear terms in storm surge predictions: Effect of tide and shelf geometry with case study from Hurricane Rita. Journal of Geophysical Research. 115(C6), doi:10.1029/2009JC005285.
[15] Rossiter, J.R., 1961. Interaction between tide and surge in the Thames. Geophysical Journal International, 6(1), 29-53.
[16] Shen, J., Gong, W., Wang, H.V., 2006. Water level response to 1999 Hurricane Floyd in the Chesapeake Bay. Continental Shelf Research. 26(19), 2484–2502.
[17] Shi, J., Yang, Z., Sha, W., 2004. Discussion on relation between surge and such elements as landing location and path of tropical cyclone effected on Zhanjiang Harbor. Marine Forecasts (in Chinese). 21(1), 43-51.
[18] Weisberg, R.H., Zheng, L., 2006. Hurricane storm surge simulations for Tampa Bay. Estuaries and Coasts. 29(6), 899-913.
[19] Wolf, J., 1978. Interaction of tide and surge in a semi‐infinite uniform channel, with application to surge propagation down the east coast of Britain. Appl. Math. Model. 2(4), 245–253.
[20] Xu, H.Z., Zhang, K.Q, Shen, J., Li, Y.P, 2010. Storm surge simulation along the US East and Gulf Coasts using a multi-scale numerical model approach. Ocean Dynamics. 60(6), 1597-1619.
[21] Zhang, K.Q, Liu, H.Q, Li, Y.P, Xu, H.Z, Shen, J., Rhome, J., Smith, T.J., 2012. The role of mangroves in attenuating storm surges. Estuarine, Coastal and Shelf Science. 102, 11-23.